

## Timing corrections of the DVCS detector

M. Mazouz, P.Y. Bertin, E. Voutier

► **To cite this version:**

M. Mazouz, P.Y. Bertin, E. Voutier. Timing corrections of the DVCS detector. 2005, 9 p. in2p3-00120984

**HAL Id: in2p3-00120984**

**<http://hal.in2p3.fr/in2p3-00120984>**

Submitted on 19 Dec 2006

**HAL** is a multi-disciplinary open access archive for the deposit and dissemination of scientific research documents, whether they are published or not. The documents may come from teaching and research institutions in France or abroad, or from public or private research centers.

L'archive ouverte pluridisciplinaire **HAL**, est destinée au dépôt et à la diffusion de documents scientifiques de niveau recherche, publiés ou non, émanant des établissements d'enseignement et de recherche français ou étrangers, des laboratoires publics ou privés.

# Timing Corrections of the DVCS Detector

Malek Mazouz<sup>1</sup>, Pierre-Yves Bertin<sup>2,3</sup>, Eric Voutier<sup>1,3</sup>

<sup>1</sup>*Laboratoire de Physique Subatomique et de Cosmologie  
IN2P3-CNRS/Université Joseph Fourier  
53 avenue des Martyrs  
38026 Grenoble cedex, France*

<sup>2</sup>*Laboratoire de Physique Corpusculaire  
IN2P3-CNRS/Université Blaise Pascal  
24 avenue des Landais  
63177 Aubière cedex, France*

<sup>3</sup>*Thomas Jefferson National Accelerator Facility,  
12000 Jefferson avenue  
Newport News, Virginia 23606, USA*

---

## Abstract

The search for refined timing spectra in coincidence experiments is a key for minimizing the effects of accidental rate. This note presents the determination of the different corrections applied to the timing of the DVCS detector, based on a correlation analysis between the coincidence time and some experimental quantities measured by the HRS spectrometer.

---

## 1 Introduction

In the context of the DVCS experiment [1], the coincidence time spectrum is a measure of the difference of the time of flight between the electron in the left HRS and the photon in the calorimeter. In order to obtain an optimized determination of the clustering algorithm in the calorimeter and to reject accidentals, the highest signal to noise ratio and the smallest accessible width should be achieved. This note presents the determination of the different corrections applied to the timing spectrum that will allow to reach an optimized time spectra.

The following study has been performed using the calorimeter time as reference because of the perfectly known time of flight of the photon. The width of the time spectrum (fig. 1) has three distinct origins. In the calorimeter, this spectrum is built from the contribution of 132 blocks having different time offsets. In the spectrometer, the time information is extracted relatively to the S2 scintillator plane, more specifically the right photomultiplier tube (PMT) of the paddle that trigger off the acquisition. Since the S2 plane is made out of 16 paddles with different offsets, the width of the time spectrum is artificially enlarged. Finally, the coincidence time is also affected by the path length of the electron into the spectrometer which may vary in a systematic way.

These three contributions to the resolution of the timing spectrum are described and studied hereafter. The coincidence time deconvoluted from these effects is then discussed.

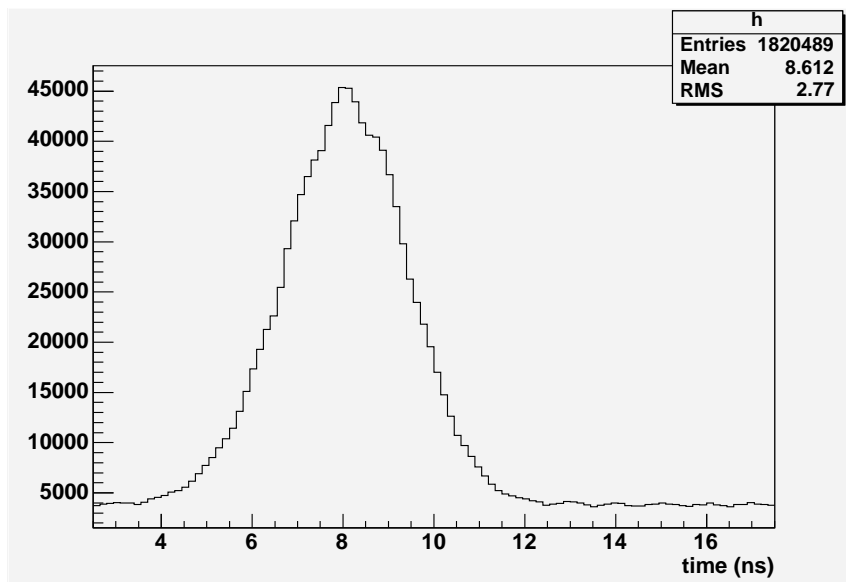


Figure 1. Raw coincidence time spectrum of the calorimeter.

## 2 Time alignment of the calorimeter

The time in the calorimeter is obtained by fitting the pulse built out of 128 ARS (Analog Ring Sampler [2]) values with respect to a reference shape depending of each single block of the calorimeter [3]. Consequently, it is equal to the difference between the arrival time of the pulse and the arrival time of the reference pulse.

This spectrum is however the sum of 132 single spectra that don't have the same average position (fig 2). This difference results from the determination method of the reference pulses and is highly connected to the choice of these pulses [3]. Because of the different mean times, the width of the coincidence

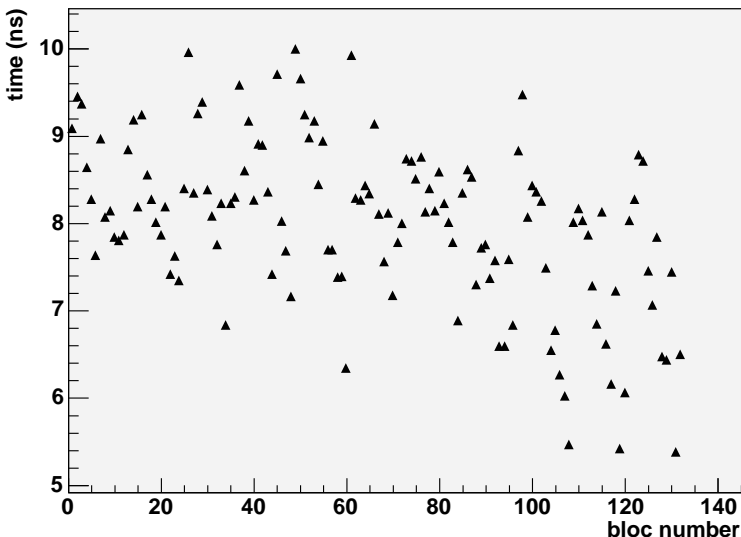


Figure 2. Mean time of the coincidence peak as a function of the calorimeter block number.

peak is effectively increased. A first time correction consists then in subtracting an artificial offset for each block in order to align at the same value (0 hereafter) the mean time of the 132 blocks. This correction allows to reduce the intrinsic width of the timing spectrum by 0.8 ns.

## 3 Time adjustment of the S2 scintillator plane

The S2 scintillator plane in the left HRS is composed of 16 paddles. Each paddle are read by two PMTs, one on each end of the paddle, the right one being used for time reference. It is then obvious that when an electron hit S2, the corresponding time in the calorimeter depends of the hit paddle and its electronic offset.

### 3.1 Determination of the trigger paddle

The selection of the trigger paddle in S2 is based on the time measured with each right PMT. It is however necessary to separate the events with respect to the number of paddle hit. Indeed, in the case of only one track in the spectrometer, the multiplicity of hit paddles can vary from 1 to several, leading to a specific identification of the paddle that trigger off the acquisition.

Fig. 3 shows the typical time spectra of a right PMT. In the case of a single hit, the trigger paddle is the only one with a non-zero time; the corresponding part of the time spectrum is the black histogram of fig. 3. In the case of a double hit, physically originating essentially from the overlap region of two adjacent paddles, the trigger paddle is the one which measured time is the closest to the reference spectrum peak (channel 1298 in fig. 3 example): the trigger paddle can be the paddle under concern or the adjacent one, generating the smaller red peak at the reference location together with its right shoulder. Events at higher time values are triggered by other paddles and correspond to high multiplicities. They originate from the cross-talk between different electronic channels and can be easily removed by a threshold on the energy deposit in the scintillator.

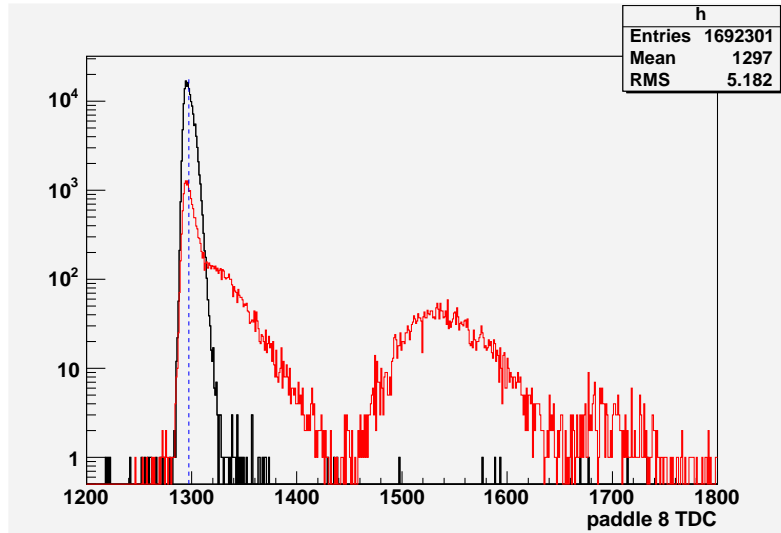


Figure 3. Time spectrum of the right PMT of paddle 8: the black part corresponds to a single hit, and the red part to double and higher hit multiplicities as explained in the text.

### 3.2 Scintillator offset adjustment

Following the previous method, the S2 paddle that trigger off the acquisition is determined on an event by event basis. Because the 16 paddles have different

electronics, it is expected that the coincidence time of the calorimeter depends of the trigger paddle. This effect is further increased by the path length of the electron in the spectrometer since each paddle covers a different region of the momentum acceptance. Fig. 4 shows the correlation between the position of the time coincidence peak, after calorimeter alignment, and the paddle number. In order to correct for this distribution, an artificial offset is added

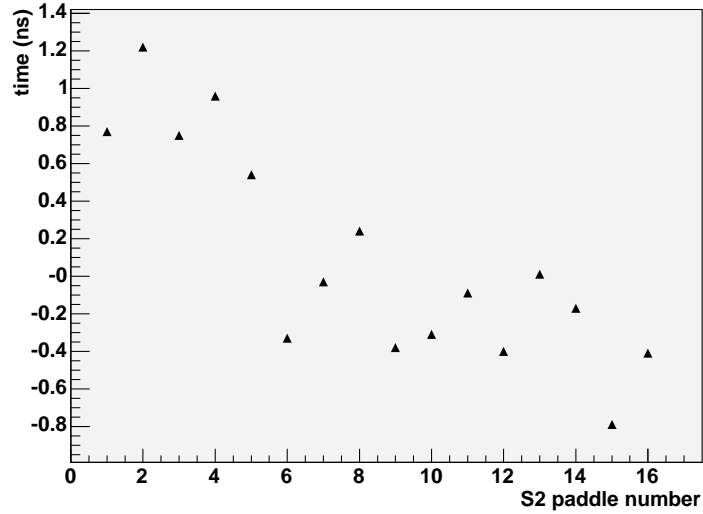


Figure 4. Coincidence peak distribution as function of the S2 paddle number.

to the coincidence time depending of the S2 paddle number.

### 3.3 Light propagation correction

The coincidence time is also depending on the location of the electron impact in the paddle. Indeed, particles travelling in the left HRS reach the S2 scintillator array in the region between -20 cm and +20 cm, in the longitudinal dimension of the paddle. The photons created in the scintillator take a certain amount of time to reach the right PMT, depending on the location of the particle impact. This time (in ns) is approximately given by

$$t = \frac{n}{c} y = 5.3 y \quad (1)$$

where  $y$  is the location (in meter) with respect to the right PMT and  $n$  is the optical index of the scintillator ( $\sim 1.6$ ). Fig. 5 shows the correlation between the  $y$  position in S2 (paddle 8) and the coincidence time in the calorimeter. As predicted, the slope of this correlation is approximately equal to 5 (Fig 6): the observed dependence as a function of the paddle may originate from the small differences between each scintillating material. The smaller slope

measured in paddle 1 is not exactly understood: it may be an effect of the reduced statistics specific of the edges of the spectrometer acceptance.

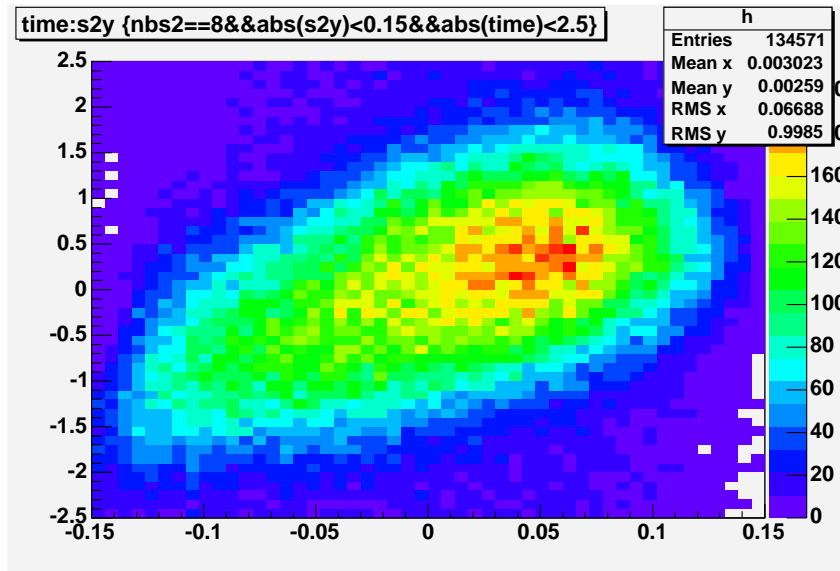


Figure 5. Time in the calorimeter versus the  $y$  position in S2 for paddle 8.

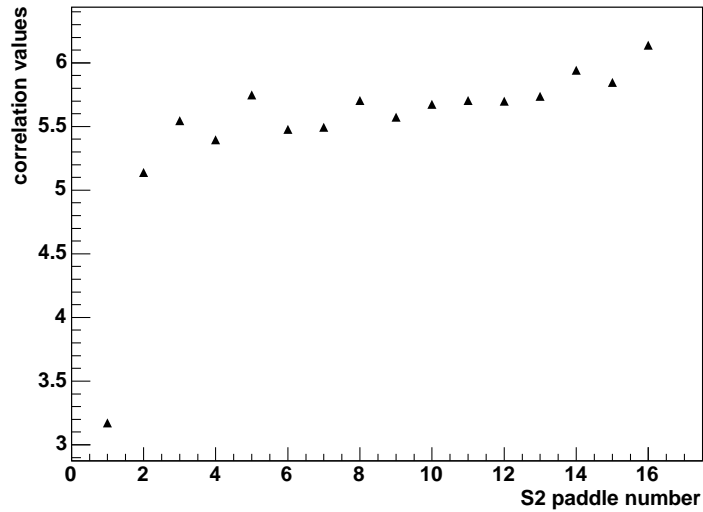


Figure 6.  $y$  position correlation slope values of the 16 S2 paddles.

To take into account this correlation, the  $y$  position in the scintillator array is determined for each event, and the coincidence time is corrected by a quantity corresponding to the product of the  $s y$ , where  $s$  is the measured slope of the correlation.

## 4 Electron path length correlation

The last correction to be applied on the coincidence time is connected to the particle path length in the left HRS. If two electrons with the same momentum travel into the spectrometer following two different trajectories, they reach S2 at two different times corresponding to their different path length. On the other side, the corresponding photons reach the calorimeter at the same moment relative to the reaction time. This discrepancy leads to different coincidence times because the acquisition is not triggered at the same instant in these two cases.

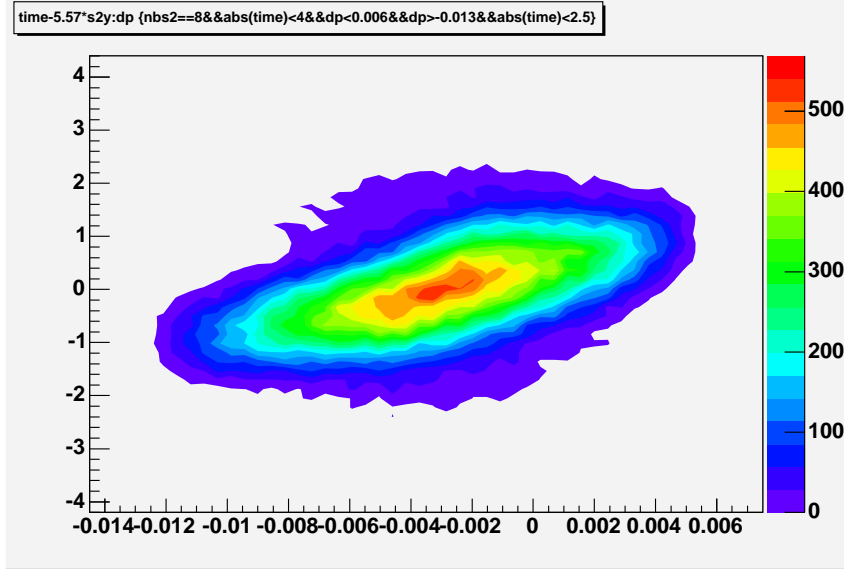


Figure 7. Coincidence time as a function of the relative HRS momentum for paddle 8.

This correlation can be studied by investigating the correlations between the coincidence time and the relative spectrometer momentum. For a given S2 paddle, the particle momentum is approximately the same, and the small variations (about 1/16 of the spectrometer acceptance) are directly connected to the trajectory length differences. Fig. 7 shows the corresponding spectra of paddle number 8: a clear linear correlation is observed which depends on the paddle number (fig. 8). In the central part of S2, the correlation is almost paddle independent while it strongly differs in the edge regions. This may be due to second order effects appearing via optical aberration in the spectrometer which develops at the edge of the acceptance.

Following the same technique as for the  $y$  position correlation, the coincidence time is corrected by a quantity  $s' \delta p/p$ , where  $s'$  is the measured correlation slope.



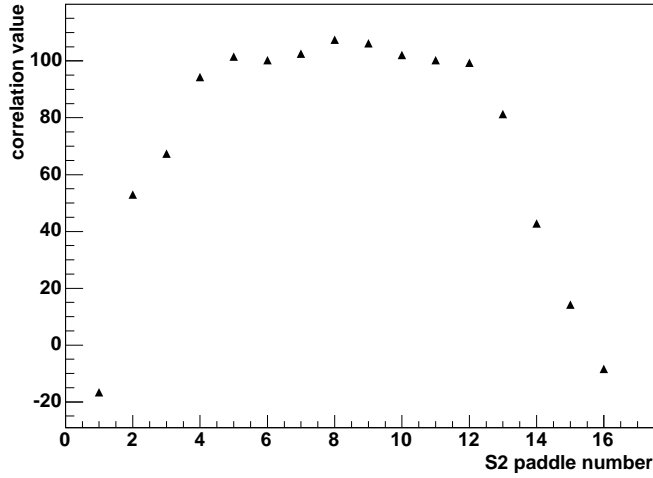


Figure 8. Momentum correlation values of the 16 S2 paddles.

## 5 Corrected coincidence time

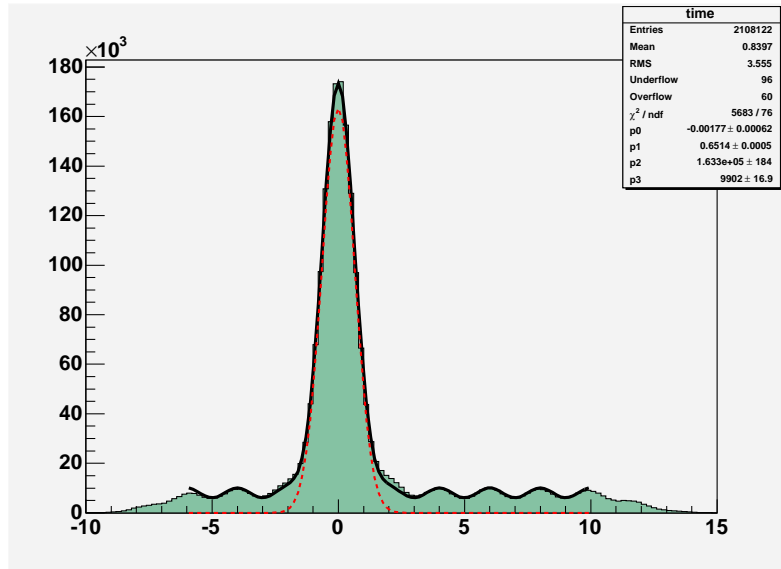


Figure 9. Coincidence time spectrum of the calorimeter after implementing the different corrections discussed in the previous sections.

Fig 9 shows the coincidence time of the calorimeter after applying all the previous corrections. The  $\sigma$ -width of the coincidence peak is about 0.65 ns as compared to an initial value larger than 1.5 ns. The fluctuations of the background are actually connected to the time structure of the JLab electron beam. They represent the sum of gaussians with the same width as the coincidence peak and separated by 2 ns:

$$T = A e^{-\frac{(x-0)^2}{\sigma^2}} + B \sum_{i=\min}^{\max} e^{-\frac{(x-2i)^2}{\sigma^2}} \quad (2)$$

where  $A/B = 16.5$ .

The previous time spectrum was obtained by assuming an energy deposit higher than 300 MeV in each block. It should be noticed that the resulting width depends on this parameter [4], as a result of the combined effects of the signal analysis method and the large background of small energy photons.

## 6 Conclusions

The study of the correlations between the coincidence time and some spectrometer measured quantities allows to reduce the accidental rate in all DVCS detectors. In fact, the previous spectrometer corrections are calorimeter independent and can be applied on all the DVCS detectors: calorimeter, proton array, and tagger.

The width of the corrected time spectrum depends on the applied energy threshold and the block position relatively to the beam, but in all cases the width of the coincidence peak and the signal to noise ratio signal are improved by these corrections. These figures are also strongly depending on the analysis method of the signal and would benefit of any improvement of the current wave form analysis.

## References

- [1] Jefferson Lab Experiment **E00-110**, P. Bertin, C. Hyde-Wright, R. Ransome, F. Sabatié spokespeople, (2000);  
Jefferson Lab Experiment **E03-106**, P. Bertin, C. Hyde-Wright, F. Sabatié, E. Voutier spokespeople, (2003).
- [2] F. Druillolle *et al.*, IEEE Trans. Nucl. Sci. **49** (2002) 1122;  
D. Lachartre, F. Feinsein, *Nucl. Inst. and Meth. A* **442** (2000) 99.
- [3] C. Munoz Camacho, <http://www.jlab.org/~munoz/calor/>.
- [4] P. Bertin, M. Mazouz, *JLab/Hall A/DVCS Analysis Note*, to appear.